A Gas Generating System for Complex Gas Mixtures – Multifunctional Application in PTR Method Optimization and Downstream Methanol Synthesis

Corina Helene Pollok[1,‡], Christoph Göbel[1,‡], Jorge Iván Salazar Gómez[1], Robert Schlögl[1,2], and Holger Ruland[1,*]

DOI: 10.1002/cite.202200033

Supporting Information available online

The multifunctional applicability of a gas mixing system is presented within the scope of Carbon2Chem® for the simulation of steel mill flue gases and their application in downstream processes. A special focus is set on the parallel operation of the gas mixing system to enable PTR-MS method optimization and methanol synthesis with simulated real gas matrices. Information is gathered for the design of downstream processes and their application, where methanol synthesis is chosen as a model reaction. A proof-of-principle study is presented where operation of a catalytic reactor setup in combination with the gas mixing system and a compressor generate reproducible results. The addition of potential trace components in methanol synthesis is exemplarily demonstrated using ammonia. With respect to the PTR-MS application, the dosing of two calibration gas standards, toluene and carbonyl sulfide, via the gas mixing system were analyzed in detail. The obtained results give insight into its applicability to simulate traces and enables the further development of analytical methods for the analysis of trace impurities in the ppb and ppt range in complex gas mixtures.

Keywords: Methanol synthesis, Proton transfer reaction, Steel mill flue gases, Trace impurities

Received: March 11, 2022; *revised:* May 05, 2022; *accepted:* May 27, 2022

1 Introduction

The increasing energy demand and the related shortage of fossil fuels require ecologically friendly alternatives on the background of the ongoing climate change [1–3]. Thus, not only the development of renewable energy sources has to be promoted but also the transformation of existing technologies applying suitable carbon capture and utilization (CCU) strategies regarding their contribution by emission, e.g., steel production plants, which emit large amounts of CO_2-rich gases [4, 5]. Within the scope of the project Carbon2Chem® the process gases of steel production plants serve as the starting point. Prior to application an appropriate preconditioning has to be configured in order to utilize the flue gases as a chemical feedstock, which is demanding as demonstrated in [6] discussing the variability of the originating process gases. Beside main components the composition of the included trace components play a crucial role and so far, there is only limited information in the ppb or ppt concentration range in the entirety of the steel mill flue gases. [7–9]

Beside the main components, the steel mill flue gases contain numerous traces [10, 11]. Thus, an elaborate gas cleaning is needed to remove typical trace components, especially sulfur-containing components and other potential components that may act as a selective catalyst poison in a downstream application depending on the desired catalytic reaction and the nature of the catalytically active sites

[1]Dr. Corina Helene Pollok‡, Dr. Christoph Göbel‡, Dr. Jorge Iván Salazar Gómez, Prof. Dr. Robert Schlögl, Dr. Holger Ruland
holger.ruland@cec.mpg.de
Max-Planck-Institut für chemische Energiekonversion, Stiftsstraße 34–36, 45470 Mülheim an der Ruhr, Germany.

[2]Prof. Dr. Robert Schlögl
Fritz-Haber-Institut der Max-Planck-Gesellschaft, Faradayweg 4–6, 14195 Berlin, Germany.

‡ These authors contributed equally to this work.

[12–15]. Since a complete removal is cost intensive, research is conducted on the types of trace impurities and their effect on a potential downstream application.

Online monitoring of traces in the concentration ranges of ppb and ppt is of great importance since offline measurement may induce fluctuations in gas composition. It has been previously shown that a time-resolved information on trace compounds can be achieved applying a highly sensitive proton transfer reaction mass spectrometer (PTR-MS) [16]. The advantage of this technique is the possibility to quantify compounds without the need of a prior calibration. As a semi-quantitative technique, it enables online monitoring of volatile organic compounds (VOCs) using chemical ionization, and most important without the need of a preseparation by, e.g., gas chromatography. This technique usually uses hydronium (H_3O^+) cations as reagent ionization ion and supports the "soft" ionization method. A more detailed description can be found in the Supporting Information. [9, 16–26]

Due to the soft ionization molecules do not undergo a high fragmentation, leading to the fact that molecules can be detected by their molecular mass plus H^+ [27]. Further advantages of PTR-MS are that no sample preparation is needed, a higher mass range is available compared to conventional mass spectrometers, a complete mass spectrum is detected within a second and a higher mass resolution and sensitivity is given, which multiplies the analytical information contained in the spectra. [28]

Although complex gas mixtures can be analyzed with this technique, it has to be considered that the detection of isomers is not possible and the determination of isobars is extremely challenging depending on mass resolution and additionally, the presence of parasitic ions such as NO^+ and $O_2^{+\bullet}$ can enable undesired reactions [29]. The application within this work is to combine PTR-time-of-flight(TOF)-MS with a gas mixing system to identify effects of the composition of gas matrices. Since PTR-TOF-MS is a new type of technique and mostly used for air measurements, there is no database available to compare the resulting spectra with. Therefore, calibration of measurement instruments as well as the validation of analytical procedures have to be considered constantly.

Since the carbon content of steel mill flue gases provides a suitable feedstock for methanol synthesis by the addition of hydrogen from electrolysis the reaction represents a suitable industrial downstream application that is well-established. Regarding the industrial application there is an optimum in synthesis gas composition for the application of the commercial Cu/ZnO catalyst containing both, CO and CO_2, leading to a formate-based reaction pathway starting from CO_2, while CO serves as a scavenger via the water-gas shift reaction (WGSR) effectively reducing the water content. In contrast, in pure CO_2 hydrogenation water formation is of higher significance due to the reaction stoichiometry and is also depending on the recycle introducing CO formed via reverse water-gas shift (RWGS). [30–32]

Beside a complex reaction pathway, studies regarding potential catalyst poisons in the industrial case mainly focus on S-compounds leading to irreversible poisoning effects due to the formation of sulfides. Nevertheless, studies on different catalyst poisons are available for liquid phase methanol synthesis focusing on sulfur species such as COS, CS_2 and thiophene leading to irreversible catalyst degradation while apparently HCN and ammonia-related derivates show no influence. [33]

New studies demonstrate the pulse dosing of such N compounds at high pressure but do not investigate the effects on a long-term scale [34]. At the short-term scale, no significant influences are apparent, which is related to the observation that only surface sites related to methanol formation and the stabilization of related intermediates are involved, while hydrogenation sites are not affected, and thus methanol yield is only temporarily diminished. Experiments that exceed short time scales have been conducted by Schühle et al. [35], however an indium-based catalyst system was used, which does not allow direct correlation compared with the Cu/ZnO catalyst.

Within this study a process combination is demonstrated, where gases mixed at atmospheric pressure simulate the preprocessed steel mill flue gas which, subsequently, are compressed and utilized in a lab-scale methanol synthesis plant (Fig. 1). A proof-of-principle study is supported by a measurement using the selective addition of ammonia to the premixed synthesis gas revealing their effect on the catalyst activity at a first glance. [34]

In addition, the complex gas mixing system is used to introduce trace components evaluated by PTR-TOF-MS to enhance method optimization such as organic (e.g., toluene) or sulfur components (e.g., COS). Furthermore, method optimization is demonstrated considering suitable background measurements including the influence of setup parameters and atmospheric moisture contents, which can be effectively controlled with the gas mixing system. This procedure is necessary to identify and quantify trace components while measuring real gas matrices. Overall, this study supports the complementary real gas measurements. [12, 36]

2 Experimental

2.1 Gas Mixing System

The gas mixing system was introduced thoroughly in [9] demonstrating the basic layout and potential application. In the following, modifications are described to equip the existing design with additional features in order to connect the setup with a compressor unit and attached downstream applications.

Since flow ranges needed to be adapted for the main components, additional mass flow controllers were added to provide an enhanced variability of the gas mixture. The modifications are shown in Tab. 1, where an overview over

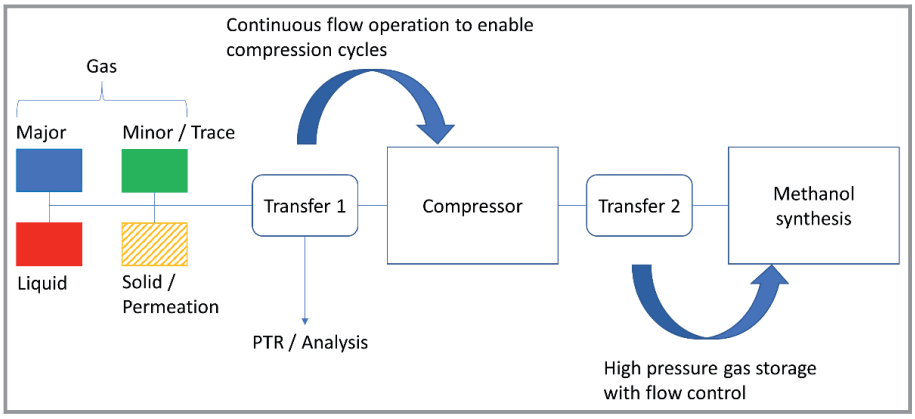

Figure 1. Schematic block chain of the process concept described in this study.

Table 1. Flow option for the main components (skid 1) of the modified mixing system. Composition ranges given in percent referred to a total flow of 1 L min^{-1}.

Gas	Flow[a)] [cm^{3}min^{-1}]	Vol%$_{min}$	Vol%$_{max}$
He	6–300	0.6	30
H_2[b)]	14–1000	1.4	100
N_2[b)]	4–1000	0.4	100
CO[b)]	1.4–500	1.4	50
O_2[b)]	0.02–30	0.002	3
CO_2[b)]	0.4–400	0.04	40
CH_4	7–350	0.7	35

a) MFC setpoint 2–100 %; b) multiple flow controllers used.

the gas types and corresponding flow ranges is given. Thus, a synthesis gas of a standard composition required for methanol synthesis can be mixed and delivered at a flow rate of 1 L min^{-1}. The synthesis gas composition applied here comprises 13.5 % CO, 3.5 % CO_2 and 73.5 % H_2 with 9.5 % N_2 added for balance and internal standard reference. The chosen composition originates from agreements with the industrial partners to establish industrially relevant conditions. Fig. 2 illustrates the modular character of the setup composed of skid 1 and 2 for main and minor components. Skid 3 houses the HovaCal®-N 17837-VOC setup for gas dosing and the addition of liquid components. Skid 4 contains the gas distribution unit, which enables multiple options. Herein, skid 1+2, skid 3, the permeation device and the oxygen feed line can be controlled separately and used for the two mixing sections, namely analytic section (blue) and compressor line (black). Both circuits can be switched to a shared exhaust line for flushing options. The analytic line features the connection of the PTR-TOF1000 in series with a GC (Agilent 7890B), which is used for the main component gas analysis. The compressor line leads to the air-driven two-stage gas compressor. This layout of the mixing section enables the option of operating both, the compressor line and the analytic circuit, independently in parallel with the required devices. Practically, in most cases this means operation of the PTR-TOF-MS using the HovaCal®-N 17837-VOC while using skid 1+2 to feed the compressor line.

The coupling of the gas mixing system to the compressor was a challenging task since the mass flow controllers

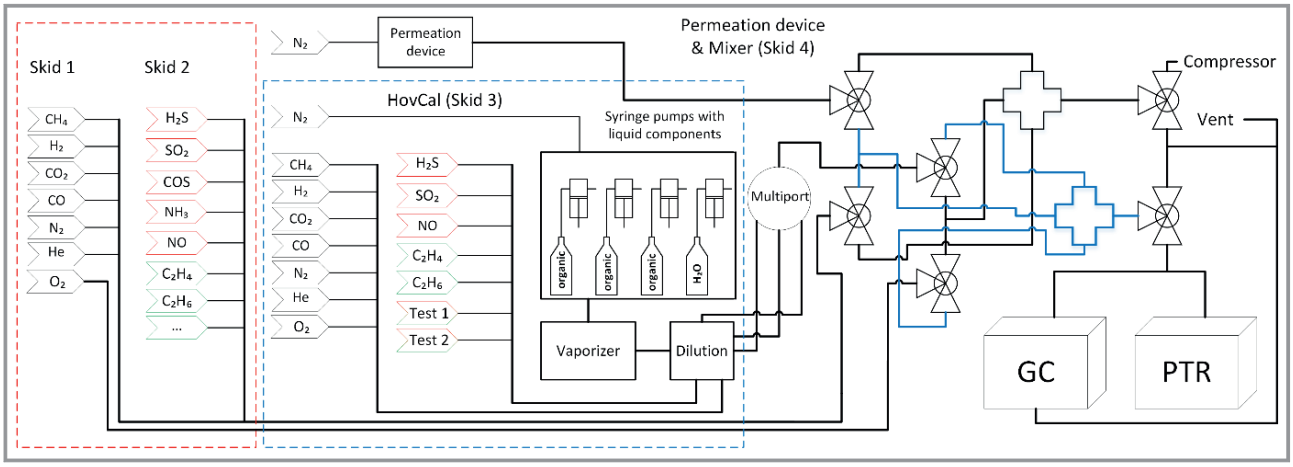

Figure 2. Schematic illustration of the gas mixing system for the dosing of gaseous, liquid and solid trace components into a main gas feed and mixing section located in skid 4 for the selection and distribution of different devices and corresponding gas streams. A declaration of symbols can be found in Fig. S1.

require a continuous flow environment for a stable operation. Thus, a transfer unit (Fig. 3) was designed which features a 20-L stainless-steel vessel constantly fed by the mixed gas stream. A bypass outlet of the container is attached to the exhaust line including a 0.7-barg check valve (10 psi, Swagelok), which provides a slight overpressure in the storage vessel. This ensures the availability of the required amount of mixed gas for compression since it is achieved in cycles on demand.

The air-driven synthesis gas compressor unit (Swagelok/RAiTec Anlagenbau, Neuss, Germany) is illustrated schematically in Fig. 3 indicating a two-stage design using gas boosters (Haskel, USA) with different compression ratios. The first stage compresses the feed from atmospheric pressure to about 5–7 bar of working pressure for the second stage. A 1000-cm^3 storage volume between both enables the effective decoupling of the stages and ensures a sufficient gas volume in the system. Control of the stages is achieved by electronically actuated needle valves effectively regulating the compressed air supply for both stages. The interplay of both pressure stages is adjusted by a set of parameters within the compressor control panel (WinCC, Siemens). Any occurring failure in the feed section or the receiving installation, which would lead to a drop in the desired working pressure, automatically forces the system into an auto shutdown due to a programmed timeout for reaching the set working pressure. The system is automatically vented because a valve in normally open position is actuated upon shutdown of the compressed air supply.

The receiving side is located in the reactor setup containment and consists of a 1-L stainless-steel container leading into a pressure reducer attached to a Coriolis flow meter. A series of strategically located check valves along the synthesis gas line ensures the forward flow direction and retention of system pressure in case of events that lead to a pressure drop in a subunit.

2.2 Catalytic Reactor Setup

Methanol synthesis was conducted in a lab-scale flow setup equipped with a fixed bed reactor. The commercial setup was modified regarding the feed gas section. This leads to the option of either mixing the desired synthesis gas with the individual gas lines (CO, CO_2 H_2, N_2) fed by the laboratory gas grid (high pressure) or using the compressor to utilize gas mixtures provided by the gas mixing system (low pressure). The flow scheme of the modified setup is shown in Fig. 4.

Both gas feeds can be switched during the measurement by a three-way gas selector valve. The feed gas flows are optimized to a maximum flow rate of 500 mL min^{-1}. The internal gas mixer contains mass flow controllers for the individual gases, while the compressor line features a Coriolis flow meter which can be calibrated more easily regarding different synthesis gas compositions. The 0.5-inch reactor is housed in a single zone laboratory furnace with an isothermal zone of approx. 5 cm. Temperature control is provided by a thermocouple located in the axial center of the catalyst bed. The used reactor type can hold 1 g of catalyst loading leading to a bed length of approx. 1.2 cm. For the experiments conducted within this work the amount of catalyst was reduced to 500 mg, where inert SiC was used (700 mg) to retain the original catalyst bed length for a correct placement of the thermocouple. The catalyst bed is fixed in the reactor using quartz glass rods of a defined length and a

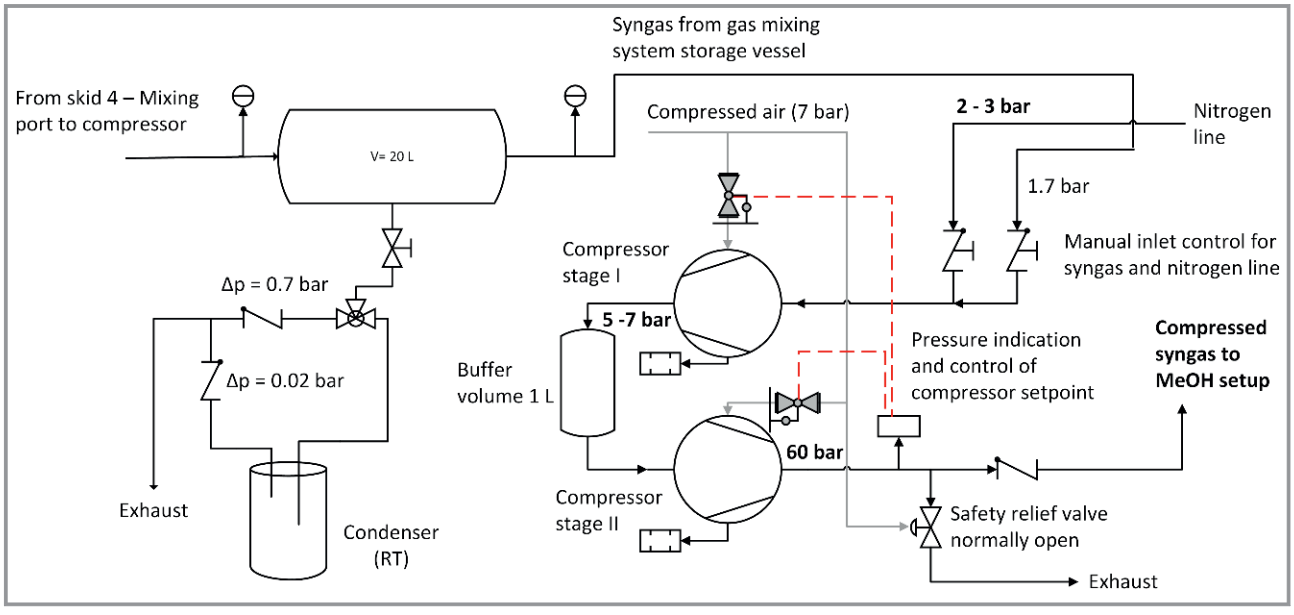

Figure 3. Transfer unit for continuous flow operation and flow scheme of the compressor unit. A declaration of symbols can be found in Fig. S1.

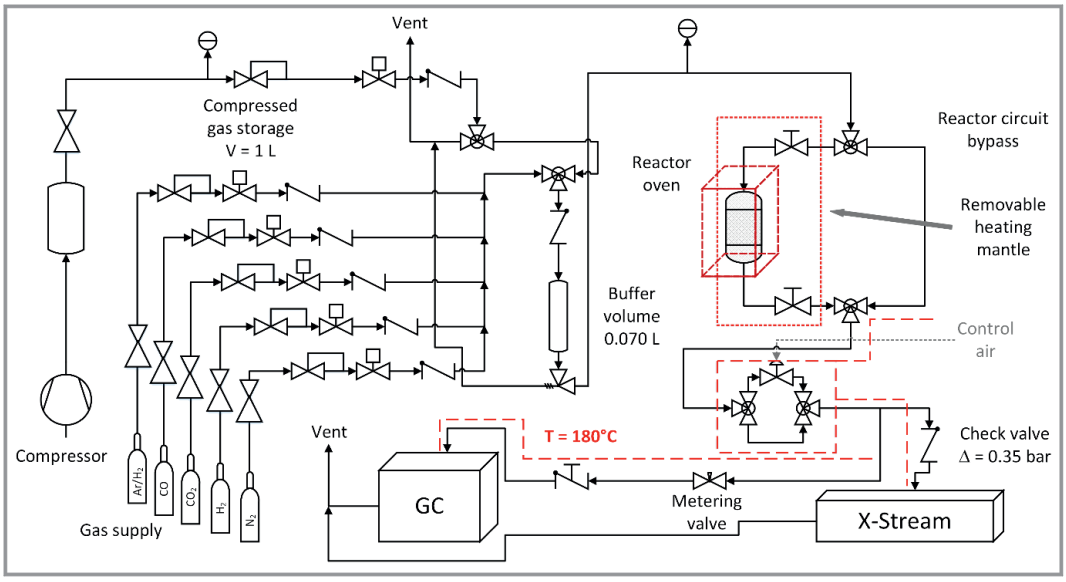

Figure 4. Flow scheme of the modified reactor flow setup for methanol synthesis. A declaration of symbols can be found in Fig. S1.

defined amount of quartz wool. This effectively reduces the dead volume and enables the reproducible packing of the reactor for each experiment. The procedure and parts used for the stabilization of the catalyst bed are shown in a schematic drawing in Fig. S2 (Supporting Information). Product gas analysis is achieved using a combination of fast IR gas analysis (Emerson X-Stream) and gas chromatography. The IR detector has four channels analyzing CO, CO_2, methanol and water. It has to be considered that the indicated concentrations are not volume corrected. In addition, gas chromatography is used for quantification due to the possibility of volume correction. The used instrument (Agilent 7890B) is equipped with two main gas paths leading to analysis by thermal conductivity detector (TCD) and TCD/FID combination (flame ionization detector). The flow sheet indicating the column interconnection and corresponding chromatograms are presented in Figs. S3–S5.

2.3 Methanol Synthesis

Methanol synthesis was conducted using a commercial catalyst based on a Cu/ZnO system, which was provided by project partner Clariant. Catalyst activation was performed according to a standard procedure [32] consisting of a two-step activation where in a first step the catalyst was heated in a flow of diluted hydrogen of 100 mL min^{-1} (2 % H_2 in Ar) to 175 °C using a heating ramp of 1 K min^{-1} and a hold time of 15 h. In the second step the catalyst is heated further to 240 °C utilizing the same heating ramp and a hold time for 30 min. First tests were conducted using benchmark conditions, which were defined to 250 °C, 50 bar and 1000 mL $min^{-1}g_{cat}^{-1}$. As a synthesis gas mixture, a feed of the composition 13.5 % CO, 3.5 % CO_2, 73.5 % H_2 and 9.5 % N_2 was used, where nitrogen represents the internal standard. This composition ensures the establishment of industrially relevant conditions. The experiment conditions further include a mass related flow of 1000 mL $min^{-1}g_{cat}^{-1}$ (0.5 g catalyst loading) to avoid overheating of the catalyst bed. Otherwise, potential overheating may severely aggravate the kinetic analysis. The test sequence comprises an induction period of 100 h, which will lead to a certain degree of catalyst deactivation. Since the induction period is limited to 100 h, it has to be considered that further deactivation underlies the derived results. In the following, initial conditions are established for comparison until the gas atmosphere is switched from the internal gas mixer of the setup to the premixed synthesis gas from the compressor unit. Raw gas measurements were performed in advance and after the sequence, respectively.

2.4 Method Optimization for PTR-MS

Within the scope of the Carbon2Chem® project this work will be focused on testing the PTR-TOF1000, which is combined to the previously described gas generating system. Calibrations are performed for two gas standards, toluene and carbonyl sulfide, which are possible traces in steel mill flue gases. In addition, the importance of humidification for toluene is investigated and compared to the dry calibration gas standard measurement. To further compare the reproducibility of the system, toluene is in addition to the gas calibration standard injected as liquid, and likewise measured dry as well as humidified.

The herein used instrument for the PTR-TOF-MS measurement is the PTR-TOF1000 mass spectrometer acquired by Ionicon Analytik GmbH, Innsbruck, Austria. It has a resolution of 1000 m/Δm. A detailed description of the instrument is given by Jordan et al. [28] and Lindinger et al. [28, 37]. In this work, the measurements for toluene (proton affinity 784 kJ mol^{-1}) were proceeded with H_3O^+. The ions are generated in the hollow cathode ion source using water vapor. The parameters for the drift tube were set to 600 V, 2.30 mbar and 80 °C, which gives an *E*/*N* value of 131 Td (Townsend, equals 10^{-17} V cm^2). The inlet temperature was set to 80 °C. For carbonyl sulfide (proton affinity 628.5 kJ mol^{-1}) measurements were performed with $O_2^{+\bullet}$. The drift tube was set to 600 V, 2.30 mbar and 60 °C with a resulting *E*/*N* value of 129 Td. In the detection region an orthogonal acceleration in the V-mode is used. For mass range *m*/*z* 15 up to 738 was applied. For mass calibration, the internal standard (PerMaSCal, 1,3-diiodobenzene, $C_6H_5I^+$, *m*/*z* 203.943 and $[C_6H_4I_2]H^+$, *m*/*z* 330.848) and the masses of the second isotope of H_3O^+ ($H_3{}^{18}O^+$, *m*/*z* 21.022) and of NO^+ (*m*/*z* 29.997) were used for measurement of toluene. For mass calibration within the carbonyl sulfide measurement the internal standard of PerMaSCal and the masses of NO_2^+, *m*/*z* 45.992 and the second isotope of O_2^+ ($^{18}O_2^+$, *m*/*z* 33.994) were used, respectively. Data acquisition was performed applying the Ionicon software IoniTOF 3.0.55, and for data analysis the PTR-MS Viewer 3.4.2 was used (all measurement parameters are summarized in Tab. S5).

For the generation of different concentrations of the calibration gas (and also humidified gases) the HovaCAL® in skid 3 was used. This instrument can dynamically generate gas standards of typical VOCs from a few ppt up to ppm level under dry and humid conditions. Therefore, the advantage is the possibility to prepare gas mixtures from substances that are not in the pool of available substances and allows the optimization of measurement parameters of individual substances under controlled conditions (e.g., relative humidity, concentrations). It consists of an evaporation chamber, a dosing and temperature control as well as a dilution part. The liquid of interest, e.g., water in case of humidifying the gas, is injected into the evaporator via a syringe pump module and mixed with a defined carrier gas flow. The dosing range depends on the used syringe, which was in this experiment 25 µL and 250 µL for toluene and water, respectively. During the measurements the evaporators were kept at 120 °C to avoid condensation and guarantee complete evaporation inside the instrument or lines. Humidification was carried out using HPLC-grade water stored in DURAN® glass bottle reservoirs, which were connected to the gas mixing system via a tubing of few millimeters. This instrument, a multicomponent gas generating system for the injection of liquid and gaseous components is based on a 3-stage dilution concept. [38] With this dilution concept dilution ratios of up to 1:10^6 can be accomplished. An additional heating line was connected between the HovaCal gas generator and the PEEK™ line of the PTR-TOF1000 and kept constant at 120 °C. The control software is based on LabVIEW (National Instruments) and allows to regulate parameters like evaporator temperature, gas flow of the calibration gas as well as of matrix gas (N_2, usually kept at 2500 mL min^{-1}), valve switching, level of humidity (in % RH), injection rates and concentration adjustment.

3 Results and Discussion

3.1 Methanol Synthesis

To verify the suitability of the gas mixing system for the combination with a subsequent high-pressure process application, methanol synthesis was investigated with both, the internal gas supply of the catalytic reactor setup as well as a gas mixture provided by the gas mixing system via the compressor unit. Fig. 5 shows the induction period using the

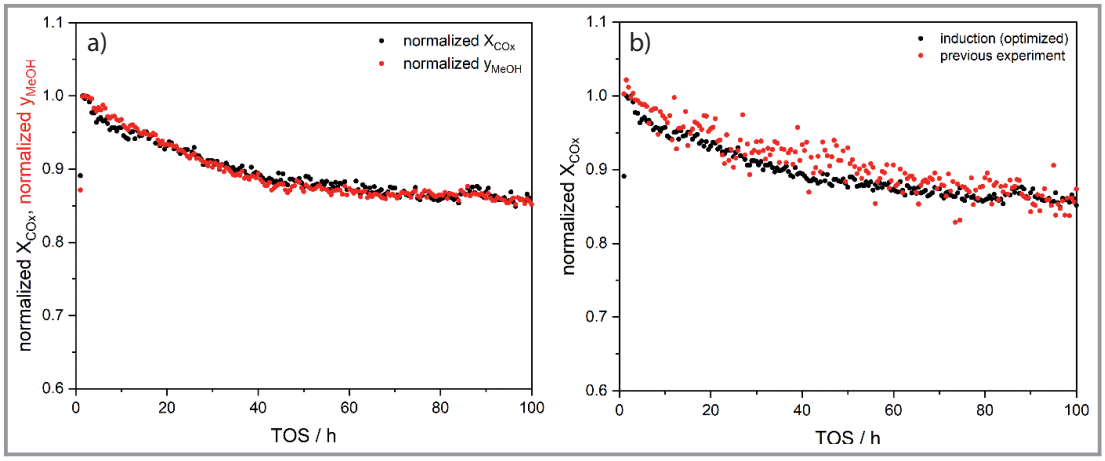

Figure 5. a) Normalized CO_x conversion and normalized methanol mole fraction for the first 100 h TOS. b) Comparison of induction period under initial and optimized conditions. Reaction conditions: 250 °C, 50 bar and 1000 mL min^{-1}g$_{cat}^{-1}$.

internal gas mixer of the lab-scale flow setup. A significant deactivation can be observed within the first 100 h time on stream (TOS), which amounts to about 85 % of the initial activity.

The similar progression of the CO_x conversion as well as the methanol mole fraction indicate a well-working system, which is supported by the determined closed carbon balance. Such a strong initial deactivation predominantly induced by thermal sintering is typical for Cu/ZnO catalysts under these conditions. [39]

However, it has to be considered that a further deactivation is observed. This is of interest for kinetic investigations, where an underlying deactivation may influence the obtained results significantly. Accordingly, an induction period of 100 h is an approach to a fast induction, where further deactivation can be accepted.

A preceding experiment was considered to estimate the reproducibility of measurements in the lab-scale synthesis setup (Fig. 5b). The experiment was conducted under the identical conditions, but in between an optimization of the regulating parameters was realized to significantly improve data quality. By enlarging the regulation cycles of the pneumatically actuated pressure regulator valve the short-term pressure and flow fluctuations could be reduced leading to a significantly smoothed trend of the measured values. Despite the high fluctuations for the preceding measurement this comparison indicates a similar progression of the deactivation in both experiments proving the downstream methanol flow setup as reproducible in standalone operation. Furthermore, the adjustment of parameters led to an acceptable data quality.

In the next step the focus was put on the air-driven synthesis gas compressor and its regulating behavior. This is more complicated compared with the internal gas supply since more flow control devices and storage volumes are involved. The complication is further expressed by the residence time behavior, which was experimentally determined as shown in Fig. S7. The residence time behavior is similar to a cascade of ideal CSTRs with $N = 3$ and a mean residence time of $\theta = 12\,800$ s according to Eq. (S6). Thus, a complete change of the atmosphere without intermediate flushing takes approximately 12 h. As a consequence, fast atmosphere changes are hampered as a proper flushing of the subunits is required. However, atmosphere changes can be performed by an interplay of both synthesis gas sources, the internal gas supply of the catalytic reactor setup and the gas mixing system, which is discussed in the following.

Both synthesis gas sources were evaluated regarding the reproducibility and the stability of their composition by comparing the measurements of several raw gas sequences and compressor test runs applying the same nominal composition (Fig. S8, S9). The overlay of chromatograms from both gas supplies indicates that not only the compositions of both mixtures are similar in the range of a reasonable measurement error but also that no oxygen is introduced by the air-driven compressor unit. Oxygen, which would appear as a peak between H_2 and N_2 in the chromatogram, would lead to a catalyst degradation, because the active state of the methanol synthesis catalyst is sensitive to oxygen traces. [14]

As a consequence, the methanol yield would drop severely as oxygen would induce an accelerated deactivation compared to the naturally occurring induction behavior. The stability of the compressor synthesis gas was further monitored over two days where multiple measurements were conducted. The results of this experiment are given in Tab. 2 and Fig. S9b. The measured average composition is similar to the desired standard composition and the standard deviation is comparably small for the single components.

Table 2. Synthesis gas provided by the gas mixing system/compressor combination. Average values from data collected over two days shown with corresponding standard deviation.

Component	Ø mixer [%]	SD [%]	Ø setup [%]	SD [%]
H_2	73.79	0.37	74.29	0.45
N_2	9.55	0.18	9.28	0.16
CO_2	3.44	0.05	3.33	0.06
CO	13.22	0.20	13.10	0.23

Thus, both synthesis gas sources are comparable while taking the potential error sources into account. Small deviations have to be tolerated since fluctuation of the mass flow controller have to be considered as well as the measurement and integration accuracy and the occurring error thereof. Furthermore, beside the multiplicity of components regarding flow control, which is different for both synthesis gas sources, it has to be considered that the systems work at different feed pressures.

As a follow-up to the induction period shown in Fig. 5a, a temporal switch to the compressor synthesis gas source was performed to verify the consistency of both gas supplies (Fig. 6a). Despite small fluctuations in the transition range induced by pressure differences in the setup the switch between the synthesis gas sources has only a small influence on the CO_x conversion and the methanol mole fraction. The evenly ongoing deactivation indicates that the composition of both mixtures matches the desired composition as demonstrated in the previous synthesis gas comparison and does not carry significant amounts of oxygen, since any unexpected deactivation is absent. In addition, the carbon balance remains stable and the return to initial conditions is achieved without disturbance.

The results of a stable and reproducible compressor application led to the first dosing experiments using NH_3 as a literature-related reversible poison for test purpose. The desired amount of NH_3 was dosed via the gas mixing system into the synthesis gas stream fed to the compressor. The catalyst used for this dosing experiment was similarly

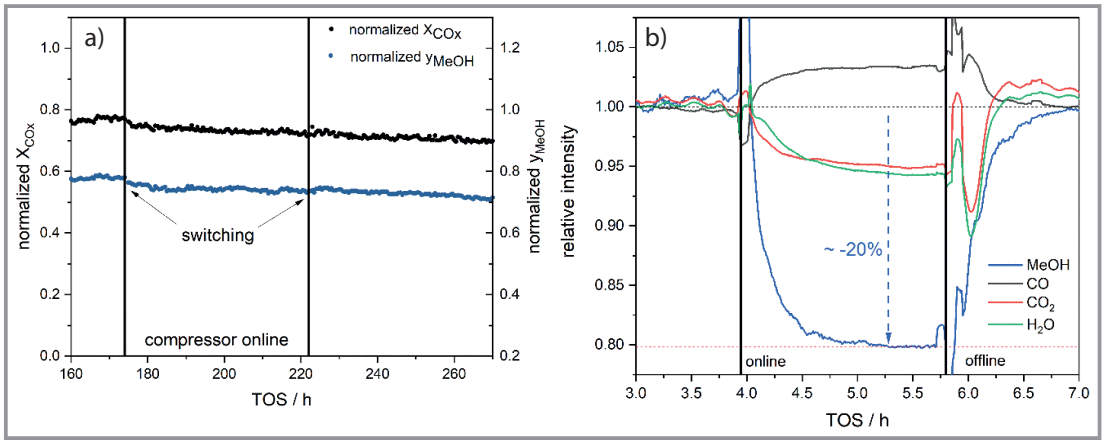

Figure 6. a) Normalized CO_x conversion and methanol mole fraction for the compressor switching experiment including induction period and return to initial conditions. Methanol mole fraction shown with offset. b) First experiment of ammonia dosing (3000 ppm in synthesis gas) using the fast response of the IR detector.

induced for 120 h before the compressor synthesis gas was switched online. Fig. 6b shows the dosing experiment recorded with the fast response IR detector. The observed spikes shortly after the switch to compressor gas result from short pressure fluctuations and flow interruptions. A relatively fast response indicates that the dosed NH_3 (3000 ppm) diminishes the methanol concentration by approx. 20 % compared to the initial value accompanied by a subsequent increase in CO concentration as a result of a reduced conversion. A new steady state is achieved after about 1 h of dosing as the methanol concentration stabilizes. Under these conditions surface sites related to methanol formation and the stabilization of intermediates thereof are involved where NH_3 is converted into methyl amines, reducing the amount of methanol formed [34]. The return to initial conditions and a clean synthesis gas by the internal gas supply of the catalytic reactor setup features a complete recovery to the initial concentration.

This experiment proves the feasibility of a selective addition of desired catalyst poisons and the effortless switching between the synthesis gas sources. Thus, long-term dosing experiments are in the range of possibilities while investigating the recovery under clean conditions is another attractive option. Overall, the process concept is a promising tool for further investigations on these topics. The investigations on methanol synthesis lead on to the second task to be achieved with the gas mixing system, namely the simulation of real gas matrices and their analysis with PTR-MS.

3.2 Trace Analysis with PTR-MS

To test the gas mixing system with the combined PTR-TOF1000 setup, a toluene calibration gas standard was used as it serves as a good benchmark compound. To validate the results of the calibration gas standard, toluene was afterwards also injected via the liquid phase to compare the reproducibility of generating the toluene vapor from the two different aggregates. Toluene belongs to the group of VOCs and has a nonpolar character and a proton affinity of 784 kJ mol^{-1} [40]. This lies in between the proton affinity of H_3O^+ (691 kJ mol^{-1}) and the first water cluster $[H_2O]H_3O^+$ (808 kJ mol^{-1}) [41]. Protonation from only the H_3O^+ ion should, therefore, be experienced without any problem. First, toluene (AirLiquide, 100 ppb in N_2 ± 10 %) was measured under dry conditions, which is principally the standard approach while mixing gases. However, to validate the herein simulated data with real gas mixtures from steel mill emissions, compounds or moreover gas mixtures also have to be remeasured under humid conditions, since only in this way impurities and reasons for the deactivation of catalysts can be detected in detail. [29, 42, 43]

Before analyzing the obtained data, the signal has to be normalized to the obtained values of the reagent ion. Therefore, the ion signal of RH^+ is normalized to the primary ion (H_3O^+) signal of 10^6 counts per second (cps) (Eq. (1)) [44]. The respective PTR-MS sensitivity towards a VOC is usually defined as the signal intensity per known volume mixing ratio.

$$ncps(C_7H_8) = \left[\frac{\text{Corrected Counts}(C_7H_8)}{(\text{Corrected Counts}(H_3^{18}O)]}\right] \cdot 10^6 \qquad (1)$$

Fig. 7 shows the results of the time series of the recorded spectra of toluene ($[C_7H_8]H^+$, *m/z* 93.082) calibration gas standard under dry conditions. Every change of concentration equilibrates rapidly and for the measurement cycles a stable signal of the substance could be determined (Fig. S10). The resulting calibration points show with an error of only 2 % almost no deviation and the points from going up (0 ppb to 100 ppb) and down (100 ppb to 0 ppb) are mostly overlapping. This means that the concentration of toluene given through the gas mixing system is very stable and reliable. Furthermore, memory effects of

accumulated toluene on the surface of the lines, which could falsify the concentration, can be excluded. The respective fitted curves allow a linear approximation for the whole range, which can be also seen in Fig. 7a (further details are given Fig. S11, S12 and Tab. S1). Fig. 7b shows a parity plot comparing the experimentally obtained concentration by applying the software PTR-MS Viewer for quantification to the nominal concentration. The lines are almost on top of each other showing that the error with an average of ~5 % is quite small for PTR-MS as a semi-quantitative method.

For the investigation of toluene under humid conditions, it was remeasured under identical experimental parameters but with changing the level of relative humidity. First, a new measurement series of dry toluene was carried out and directly after, 50 % RH were added in form of water via the gas mixing system. The corresponding results are shown in Fig. 8a.

In both cases (0 % RH and 50 % RH), the response of the instrument in normalized counts per second (normalized to the primary ion H_3O^+) is linear in the whole concentration range from 0 up to 100 ppb (see also Fig. S13–S16 and Tab. S2). It is important to mention that, similar to the dry measurement shown before, also during the humid measurement the signals obtained at various concentrations show only little deviation independent of the direction of concentration change (Fig. S13). Comparing both curves (toluene 0 % RH and 50 % RH, Fig. 8) with each other shows that while adding humidity the sensitivity of the PTR-MS decreases slightly. As the proton affinity of toluene is between H_3O^+ and $H_3O^+[H_2O]$, toluene reacts via proton transfer with H_3O^+ but not with the latter one.

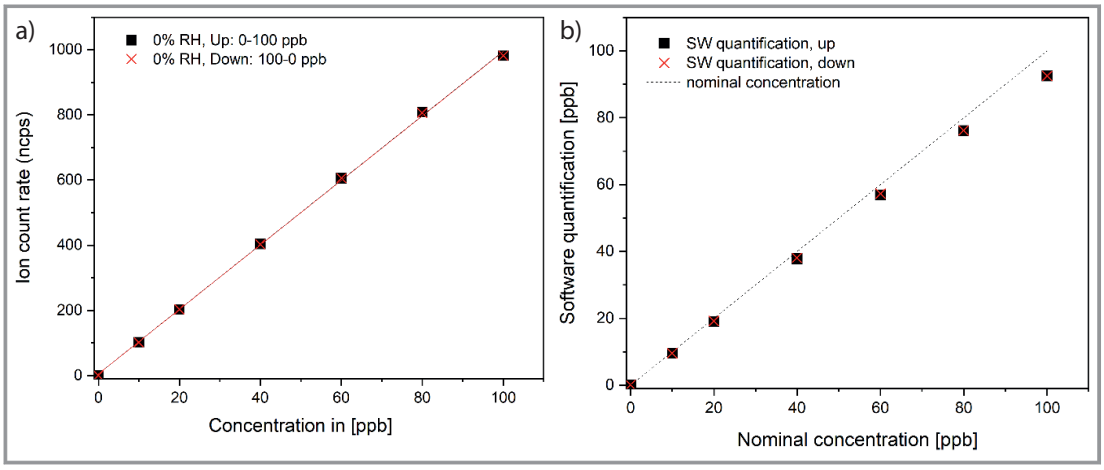

Figure 7. a) Calibration curve of toluene gas standard (dry) at different concentrations, first going up from 0–100 ppb, then down from 100–0 ppb (including linear fit). b) Parity plot of toluene gas standard (dry) measurement showing the software quantified concentration and the nominal concentration.

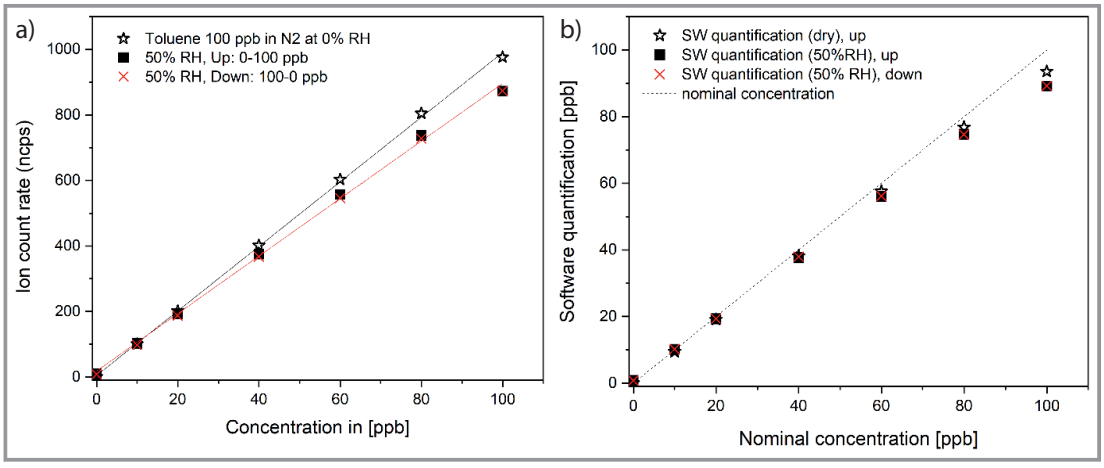

Figure 8. a) Calibration curve of toluene gas standard (dry, black star) at different concentrations going up from 0–100 ppb, toluene (50 % RH) going up from 0–100 ppb (black square) and going down 100–0 ppb (50 % RH, red cross). b) Parity plot of toluene gas standard dry (black star) and humid (squares/cross) measurement showing the experimental concentration and the nominal concentration.

Furthermore, cluster ions would complicate the spectra interpretation, which is suppressed by the use of PTR-MS due to the applied electric field, which enhances the ion kinetic energy and therefore lowers the formation of clusters. Thus, a sensitivity drop of the PTR-MS adding humidity is expected, which is defined by the slope of the linear fit of the calibration curve given in ncps ppb^{-1}. A detailed analysis of toluene regarding different levels of humidity was already carried out by Warneke et al. [42] covering the range from 20–100 % RH. Although the study presented here only focusses on 50 % RH the results are principally showing a similar trend. Nevertheless, the sensitivity itself is significantly lower. While Warneke et al. [42] obtained a sensitivity of 71 ncps ppb^{-1} for dry and around 28 ncps ppb^{-1} for humidified toluene the herein presented study only shows a sensitivity of 9.9 ncps ppb^{-1} and 8.5 ncps ppb^{-1}, respectively. The deviation in terms of sensitivity can most likely be related to the use of different instruments and instrument parameters. This is supported by the work of Beauchamp et al. [45], who used a comparable instrument as it was applied in this study and determined values in a similar range as our results.

In conclusion the herein obtained results are in agreement with the expectations. Toluene is not supposed to form clusters during the addition of water, which could be underlined here with a small sensitivity drop. A significant fragmentation of toluene could also not be observed, meaning that the humidity and the formation of water clusters did not have an influence on the fragmentation pattern, which otherwise could affect the sensitivity. [29]

After switching off the injection of toluene as well as the water injection, a signal drop is observed within less than 50 cycles, showing a low memory effect of toluene and water (Fig. S13). Fig. 8b shows the corresponding parity plot for toluene at both humification stages. The error of the experimental versus the nominal concentration is given in Tab. S2. In this second measurement series (toluene, 0 % RH) carried out under identical conditions as the first series the averaged error is with 4 % almost identical to the error of 5 % described above. This error is completely in line with the error for humid toluene (toluene, 50 % RH), which is calculated to ~5 % with respect to the ratio of experimental and nominal concentration. This shows that the measurements are reproducible and the error with being below 10 % is low for PTR-MS as a semi-quantitative method.

To further check the reproducibility and reliability of the system, toluene was additionally injected into the gas mixing system from liquid phase (toluene purchased from Sigma Aldrich, anhydrous 99.8 %) to generate the vapor in the corresponding concentrations. Likewise, the humidification was also investigated and compared in Fig. 9 similar to the previously shown results from the gas aggregate. Since the liquid phase has no limitation in comparison to the gas standard due to its concentration (calibration gas standard 100 ppb in N_2), liquid toluene could also be measured at higher concentration ranges (1000 ppb), while for the gas standard the maximum was limited to 100 ppb. The higher concentration ranges (> 100 ppb) are shown in Figs. S17–S20 to simplify the direct comparison of the different aggregates in Fig. 9.

The comparison directly shows a high reproducibility of the results towards the previously obtained values from the gas standard. The concentrations increase linearly resulting in a consistent calibration line. The concentration point of liquid toluene (50 % RH) at 100 ppb can be neglected in the analysis, since it can be explained by an instrumental change of the dilution stage and a too short equilibration time. After this change, at higher concentrations everything is back in the trend as can be seen in Fig. S18 and S19. The difference in software quantification is with a deviation of 10 % (0 % RH) and 11 % (50 % RH) slightly higher than from the gas standard, but still in a reasonable range. If

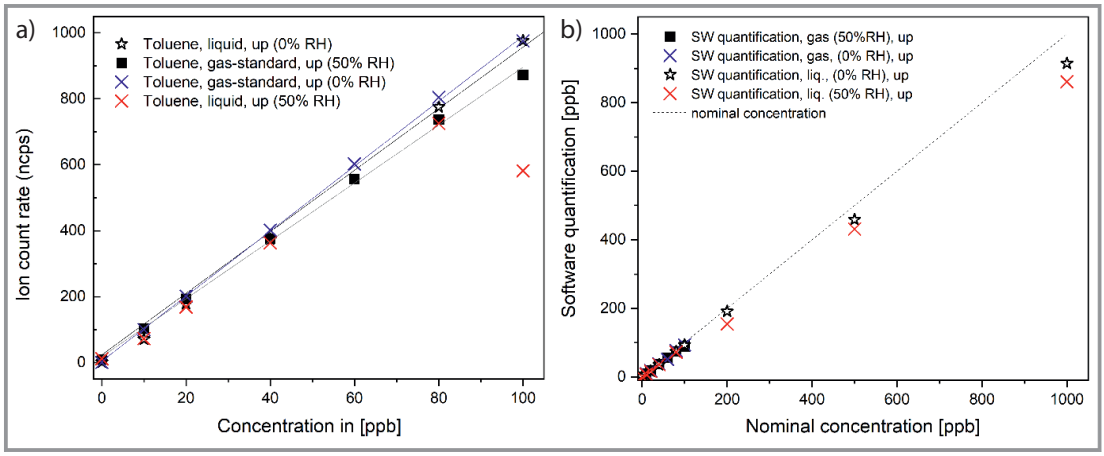

Figure 9. a) Calibration curve of toluene (liq.) (dry, black star)) and liq. (50 % RH, blue cross) at different concentrations going up from 0–100 ppb, toluene gas standard (50 % RH) going up from 0–100 ppb (black square) and gas standard (0 % RH, red cross). b) Parity plot of liq. toluene dry (black star) and from humid (50 % RH, red cross) and from gas standard dry (blue cross) and humid (50 % RH, black square) showing the experimental concentration and the nominal concentration.

focused on the sensitivity of PTR-MS towards the humidification of gases, toluene (0 % RH) generated from liquid phase results in a sensitivity of 9.3 ncps ppb^{-1}, while for 50 % RH a decrease to 8.5 ncps ppb^{-1} is observed. This sensitivity drop for humidified toluene is in very good agreement with the sensitivity values obtained from the gas standard (Tab. 3), since for both aggregates it is about 10 %.

Table 3. Overview of the different toluene injections and the level of humidity with respect to the obtained sensitivity in ncps.

Measurement type	0 % (RH)	50 % (RH)	Change [%]
1st series: calibration gas std.	9.9	–	–
2nd series: calibration gas std.	9.9	8.8	11
3rd series: liquid	9.3	8.5	9

The complementary experiments with the two different aggregates, a gas standard and liquid phase, clearly prove the functionality of the herein presented systems, and the produced results are reliable no matter how the sample is injected into the gas mixing system. A very low fragmentation is observed, and the obtained calibration line is stable and follows a linear trend even at high concentrations (1000 ppb). To further investigate samples of tremendous interest for the analysis of industrial process gases, COS is used as example for a sulfur-containing compound. A calibration using a calibration gas standard (Westfalen Gas, carbonyl sulfide 1.00 vol % in N_2 6.0) was performed as previously described for toluene. COS was introduced using the defined experimental conditions for the PTR-TOF-MS described in the corresponding section. Fig. S21 shows the time series of the recorded spectra of COS^+ (*m/z* 59.966) in a nitrogen gas matrix under dry conditions for concentrations in the range of 10 ppb to 1000 ppb (detailed values are given in Tab. S4). Since COS is a strong adsorbing compound, for each step a stable and equilibrated signal was awaited to determine the counts. Due to its proton affinity of 628.5 kJ mol^{-1} (NIST [46]), carbonyl sulfide has to be measured with $O_2^{+\bullet}$, since it has a lower proton affinity compared to water (~691 kJ mol^{-1}).

Similar to toluene under dry and humid conditions, a reliable calibration curve could be obtained (Fig. 10). The corresponding linear curve fits can be found in Fig. S22. A linear approximation was obtained for the whole concentration range from 0 to 1000 ppb. The parity plot for COS and the resulting values are shown in Fig. 10b and Tab. S4. According to the resulting averaged error a strong deviation can be obtained for COS. The concentration, which is entered into the gas generator is obviously almost doubled in contrast to the monitored concentration with the PTR mass spectrometer where only ~64 % are obtained resulting in a deviation of around 36 %. However, it has to be noted that toluene and COS are measured with different primary ions, which might influence the reported error. While toluene was measured with H_3O^+ for protonation, $O_2^{+\bullet}$ had to be used for COS due to the proton affinity of the analyte. Nevertheless, since PTR-MS is a semi-quantitative method where a usual error of ~50 % (IONICON [47] Hands-On PTR 2019) has to be considered, the here obtained error of 36 % is in an acceptable error range. Overall, the derived calibration curves indicate a reasonable small deviation when quantification is performed applying the PTR software making in combination with its high sensitivity PTR-MS a powerful tool for the analysis and quantification of complex gas mixtures.

4 Conclusions

The herein obtained results are important steps towards the analysis and application of steel mill flue gases. Within the

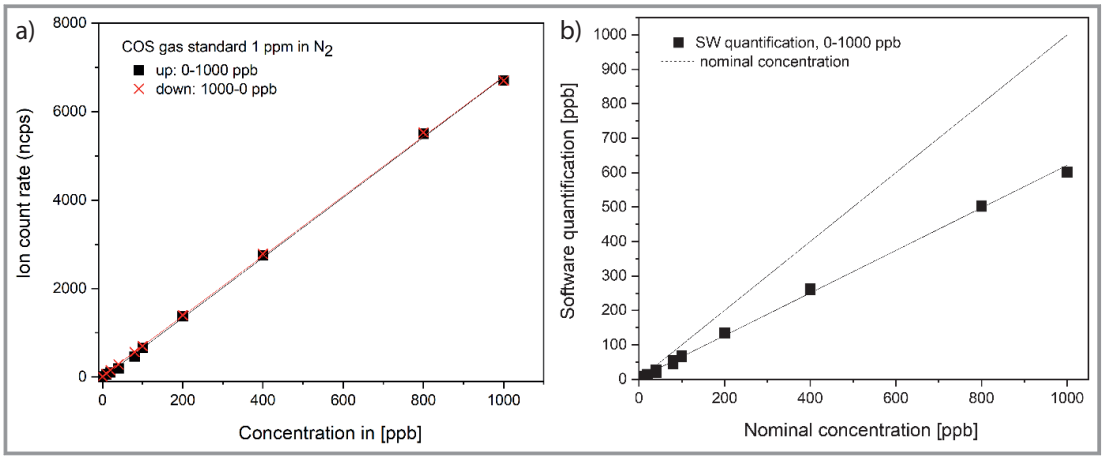

Figure 10. a) Calibration curve of COS (dry) at different concentrations, first going up from 0–1000 ppb (black square) and down from 1000–0 ppb (red cross). b) Parity plot of COS measurement showing the experimental concentration and the nominal target concentration.

here presented measurements the base was developed to further investigate gas traces at the ppb- or even ppt-level in gas matrices online and without the need of separation methods. Furthermore, the performance of the gas mixing system could be validated. Calibration curves for two compounds, toluene under dry and humid conditions, and carbonyl sulfide under dry conditions were obtained demonstrating that the herein presented setup provides a reasonable tool for method optimization in PTR-MS. In addition, the error of the used instrument (PTR-TOF1000) was obtained with parity plots, showing that depending on the analyte and measurement method (H_3O^+ vs. O_2^+) the error is of about 5 % (toluene) and 36 % (COS), which is in a good agreement with the error of ~50 % given by the instrument supplier. It has to be noted that this method allows a reasonable quantification with high sensitivity even with a detailed calibration, which is not applicable with other analytical methods like gas chromatography or conventional mass spectrometry. The presented gas mixing system combines mixing of gases, evaporation of analytes and water and the dilution of premixed gases to produce dry or humid multicomponent test gases with defined trace concentrations. It offers a wide range of possibilities to simulate gas mixtures also with toxic and corrosive analytes and to study catalytic reactions or gas purification methods. A future focus will also be directed to fragmentation patterns of different compounds in terms of generating a spectral database under controlled conditions (matrix, humidity, concentration), which is unavailable so far. This will allow to simulate and online monitor industrial process gases on an industrial scale and, therefore, support the development of gas cleaning strategies for the application of these gases in catalytic processes for the production of, e.g., methanol.

In addition, the proof-of-principle study to use the gas mixing system as a synthesis gas source for methanol synthesis is established. The coupling of three subunits (gas mixing system, compressor and catalytic flow setup) delivers comparable synthesis gas performance referred to the internal gas supply and allows the selective addition of potential catalyst poisons to the synthesis gas feed. The deviation between both sources is comparably small, despite the significantly different setups and multiplicity of components involved. The air-driven compressor can compress the synthesis gas without adding traces of oxygen, which is especially important for the investigation in methanol synthesis. Overall, a stable and reproducible operating performance is observed for these initial experiments. This enables beside short-term studies also long-term experiments, which are rarely found in literature, while also recovery studies can be performed. As a result of the modular integration in the overall process concept the design of the gas distribution section allows the generation of synthesis gas for methanol synthesis as well as for the method optimization for PTR-MS analysis in parallel, which represents an efficient approach to contemporary laboratory infrastructure on the larger scale. This is a key-step for Carbon2Chem®: online gas characterization combined with catalytic test setups to determine the use of steel mill flue gases as raw material.

Supporting Information

Supporting Information for this article can be found under DOI: https://doi.org/10.1002/cite.202200033.

The authors thank the Federal Ministry of Education and Research (Germany) (Bundesministerium für Bildung und Forschung, BMBF, Verbundvorhaben Carbon2Chem®, support codes: 03EK3037C and 03EW0004C) for funding as well as the Max Planck Society for financial support. The catalyst used in this study was kindly provided by project partner Clariant. Open access funding enabled and organized by Projekt DEAL.

Symbols used

Ai	[Area units]	GC area
E/N	[Td]	Reduced electric field
k	[–]	Collision rate
m	[g]	Mass
m/z	[–]	Mass to charge ratio
M	[g mol^{-1}]	Molar mass
N	[–]	Number of reactors
$\dot{n}$	[mol s^{-1}]	Molar flow
p	[bar]	Pressure
S	[%]	Selectivity
t	[s]	Time
T	[°C, K]	Temperature
X	[%]	Conversion
y_i	[–]	Mole fraction
θ	[–]	Reduced residence time
τ	[s]	Residence time

Abbreviations

BFG	Blast furnace gas
BOFG	Basic oxygen furnace gas
CCU	Carbon capture and utilization
COG	Coke oven gas
COS	Carbonyl sulphide
cps	Counts per second
CSTR	Continuously stirred tank reactor
FID	Fame ionization detector
GHG	Greenhouse gas
Liq.	Liquid
MFC	Mass flow controller

MS	Mass spectrometer
ncps	Normalized counts per second
PAH	Polycyclic aromatic hydrocarbons
PCB	Polychlorinated diphenyls
PerMaSCal	Permeation device for mass scale calibration
PTR	Proton transfer reaction
RH	Relative humidity
RMRi	Relative molar response factor
RWGS	Reverse water gas shift
SRI	Selective reagent ionization
TCD	Thermal conductivity detector
TOF	Time-of-flight
VOC	Volatile organic compound
WGSR	Water-gas shift reaction

References

[1] R. Schlögl, *Top. Catal.* **2016**, *59*, 772–786. DOI: https://doi.org/10.1007/s11244-016-0551-9

[2] R. Schlögl, in *CO2 und CO – Nachhaltige Kohlenstoffquellen für die Kreislaufwirtschaft* (Eds: M. Kircher, T. Schwarz), Springer, Berlin **2020**, 77–98.

[3] *Climate Change 2014 Mitigation of Climate Change* (Eds: O. Edenhofer et al.), Working Group III Contribution to the Fifth Assessment Report of the Intergovernmental Panel on Climate Change, IPCC, Geneva **2014**.

[4] J. M. Bermúdez, A. Arenillas, R. Luque, J. A. Menéndez, *Fuel Process. Technol.* **2013**, *110*, 150–159. DOI: https://doi.org/10.1016/j.fuproc.2012.12.007

[5] H. Kim, J. Lee, S. Lee, I.-B. Lee, J.-h. Park, J. Han, *Energy* **2015**, *88*, 756–764. DOI: https://doi.org/10.1016/j.energy.2015.05.093

[6] G. Deerberg, M. Oles, R. Schlögl, *Chem. Ing. Tech.* **2018**, *90*, 1365–1368. DOI: https://doi.org/10.1002/cite.201800060

[7] J.-H. Tsai, K.-H. Lin, C.-Y. Chen, N. Lai, S.-Y. Ma, H.-L. Chiang, *J. Hazard. Mater.* **2008**, *157*, 569–578. DOI: https://doi.org/10.1016/j.jhazmat.2008.01.022

[8] M. Oles, W. Lüke, R. Kleinschmidt, K. Büker, H.-J. Weddige, P. Schmöle, R. Achatz, *Chem. Ing. Tech.* **2018**, *90*, 169–178. DOI: https://doi.org/10.1002/cite.201700112

[9] J. I. S. Gómez, E. S. Takhtehfouladi, R. Schlögl, H. Ruland, *Chem. Ing. Tech.* **2020**, *92*, 1574–1585. DOI: https://doi.org/10.1002/cite.202000110

[10] P. J. Kirton, J. Ellis, P. T. Crisp, *Fuel* **1991**, *70*, 1383–1389. DOI: https://doi.org/10.1016/0016-2361(91)90003-S

[11] N. B. Coupe, W. Girling, R. P. W. Scott, *J. Appl. Chem.* **1961**, *11*, 335–343. DOI: https://doi.org/10.1002/jctb.5010110904

[12] J. I. Salazar Gómez, C. Klucken, M. Sojka, G. von der Waydbrink, R. Schlögl, H. Ruland, *Chem. Ing. Tech.* **2020**, *92*, 1514–1524. DOI: https://doi.org/10.1002/cite.202000101

[13] J. Schittkowski, H. Ruland, D. Laudenschleger, K. Girod, K. Kähler, S. Kaluza, M. Muhler, R. Schlögl, *Chem. Ing. Tech.* **2018**, *90*, 1419–1429. DOI: https://doi.org/10.1002/cite.201800017

[14] J. He, D. Laudenschleger, J. Schittkowski, A. Machoke, H. Song, M. Muhler, R. Schlögl, H. Ruland, *Chem. Ing. Tech.* **2020**, *92*, 1525–1532. DOI: https://doi.org/10.1002/cite.202000045

[15] F. Nestler, M. Krüger, J. Full, M. J. Hadrich, R. J. White, A. Schaadt, *Chem. Ing. Tech.* **2018**, *90*, 1409–1418. DOI: https://doi.org/10.1002/cite.201800026

[16] W. Lindinger, A. Hansel, A. Jordan, *Int. J. Mass Spectrom. Ion Processes* **1998**, *173*, 191–241. DOI: https://doi.org/10.1016/S0168-1176(97)00281-4

[17] F. Clementschitsch, K. Bayer, *Microb. Cell Fact.* **2006**, *5*, 19. DOI: https://doi.org/10.1186/1475-2859-5-19

[18] B. D'Anna, A. Wisthaler, Ø. Andreasen, A. Hansel, J. Hjorth, N. R. Jensen, C. J. Nielsen, Y. Stenstrøm, J. Viidanoja, *J. Phys. Chem. A* **2005**, *109*, 5104–5118. DOI: https://doi.org/10.1021/jp044495g

[19] V. I. Bukhtiyarov, A. I. Nizovskii, H. Bluhm, M. Hävecker, E. Kleimenov, A. Knop-Gericke, R. Schlögl, *J. Catal.* **2006**, *238*, 260–269. DOI: https://doi.org/10.1016/j.jcat.2005.11.043

[20] A. Lagg, J. Taucher, A. Hansel, W. Lindinger, *Int. J. Mass Spectrom. Ion Processes* **1994**, *134*, 55–66. DOI: https://doi.org/10.1016/0168-1176(94)03965-8

[21] C. Yeretzian, A. Jordan, W. Lindinger, *Int. J. Mass Spectrom.* **2003**, *223–224*, 115–139. DOI: https://doi.org/10.1016/S1387-3806(02)00785-6

[22] A. Romano, L. Fischer, J. Herbig, H. Campbell-Sills, J. Coulon, P. Lucas, L. Cappellin, F. Biasioli, *Int. J. Mass Spectrom.* **2014**, *369*, 81–86. DOI: https://doi.org/10.1016/j.ijms.2014.06.006

[23] F. Biasioli, F. Gasperi, G. Odorizzi, E. Aprea, D. Mott, F. Marini, G. Autiero, G. Rotondo, T. D. Märk, *Int. J. Mass Spectrom.* **2004**, *239*, 103–109. DOI: https://doi.org/10.1016/j.ijms.2004.07.024

[24] S. Hayward, C. N. Hewitt, J. H. Sartin, S. M. Owen, *Environ. Sci. Technol.* **2002**, *36*, 1554–1560. DOI: https://doi.org/10.1021/es0102181

[25] J. A. Sánchez-López, R. Zimmermann, C. Yeretzian, *Anal. Chem.* **2014**, *86*, 11696–11704. DOI: https://doi.org/10.1021/ac502992k

[26] B. Agarwal, S. Jürschik, P. Sulzer, F. Petersson, S. Jaksch, A. Jordan, T. D. Märk, *Rapid Commun. Mass Spectrom.* **2012**, *26*, 983–989. DOI: https://doi.org/10.1002/rcm.6173

[27] M. S. B. Munson, F. H. Field, *J. Am. Chem. Soc.* **1966**, *88*, 2621–2630. DOI: https://doi.org/10.1021/ja00964a001

[28] A. Jordan, S. Haidacher, G. Hanel, E. Hartungen, L. Märk, H. Seehauser, R. Schottkowsky, P. Sulzer, T. D. Märk, *Int. J. Mass Spectrom.* **2009**, *286*, 122–128. DOI: https://doi.org/10.1016/j.ijms.2009.07.005

[29] J. I. Salazar Gómez, M. Sojka, C. Klucken, R. Schlögl, H. Ruland, *J. Mass Spectrom.* **2021**, *56*, e4777. DOI: https://doi.org/10.1002/jms.4777

[30] S. Kattel, J. Ramírez Pedro, G. Chen Jingguang, A. Rodriguez José, P. Liu, *Science* **2017**, *355*, 1296–1299. DOI: https://doi.org/10.1126/science.aal3573

[31] X. Zhang, J.-X. Liu, B. Zijlstra, I. A. W. Filot, Z. Zhou, S. Sun, E. J. M. Hensen, *Nano Energy* **2018**, *43*, 200–209. DOI: https://doi.org/10.1016/j.nanoen.2017.11.021

[32] H. Ruland, H. Song, D. Laudenschleger, S. Stürmer, S. Schmidt, J. He, K. Kähler, M. Muhler, R. Schlögl, *ChemCatChem* **2020**, *12*, 3216–3222. DOI: https://doi.org/10.1002/cctc.202000195

[33] R. Quinn, T. A. Dahl, B. A. Toseland, *Appl. Catal., A* **2004**, *272*, 61–68. DOI: https://doi.org/10.1016/j.apcata.2004.05.015

[34] D. Laudenschleger, H. Ruland, M. Muhler, *Nat. Commun.* **2020**, *11*, 3898. DOI: https://doi.org/10.1038/s41467-020-17631-5

[35] P. Schühle, M. Schmidt, L. Schill, A. Riisager, P. Wasserscheid, J. Albert, *Catal. Sci. Technol.* **2020**, *10*, 7309–7322. DOI: https://doi.org/10.1039/D0CY00946F

[36] O. Hegen, J. I. Salazar Gómez, C. Grünwald, A. Rettke, M. Sojka, C. Klucken, J. Pickenbrock, J. Filipp, R. Schlögl, H. Ruland, *Chem. Ing. Tech.* **2022**, submitted. DOI: https://doi.org/10.1002/cite.202200015

[37] W. Lindinger, A. Jordan, *Chem. Soc. Rev.* **1998**, *27*, 347–375. DOI: https://doi.org/10.1039/A827347Z

[38] W. Vautz, M. Schmäh, *Int. J. Ion Mobility Spectrom.* **2009**, *12*, 139–147. DOI: https://doi.org/10.1007/s12127-009-0030-0

[39] J. B. Hansen, P. E. Højlund Nielsen, in *Handbook of Heterogeneous Catalysis* (Eds: G. Ertl, H. Knözinger, F. Schüth, J. Weit-

kamp), Wiley-VCH, Weinheim **2008**, 2920–2949. DOI: https://doi.org/10.1002/9783527610044.hetcat0148
[40] K. Sekimoto, S.-M. Li, B. Yuan, A. Koss, M. Coggon, C. Warneke, J. de Gouw, *Int. J. Mass Spectrom.* **2017**, *421*, 71–94. DOI: https://doi.org/10.1016/j.ijms.2017.04.006
[41] R. S. Blake, P. S. Monks, A. M. Ellis, *Chem. Rev.* **2009**, *109*, 861–896. DOI: https://doi.org/10.1021/cr800364q
[42] C. Warneke, C. van der Veen, S. Luxembourg, J. A. de Gouw, A. Kok, *Int. J. Mass Spectrom.* **2001**, *207*, 167–182. DOI: https://doi.org/10.1016/S1387-3806(01)00366-9
[43] A. Vlasenko, A. M. Macdonald, S. J. Sjostedt, J. P. D. Abbatt, *Atmos. Meas. Tech.* **2010**, *3*, 1055–1062. DOI: https://doi.org/10.5194/amt-3-1055-2010
[44] B. Yuan, A. R. Koss, C. Warneke, M. Coggon, K. Sekimoto, J. A. de Gouw, *Chem. Rev.* **2017**, *117*, 13187–13229. DOI: https://doi.org/10.1021/acs.chemrev.7b00325
[45] J. Beauchamp, J. Herbig, J. Dunkl, W. Singer, A. Hansel, *Meas. Sci. Technol.* **2013**, *24*, 125003. DOI: https://doi.org/10.1088/0957-0233/24/12/125003
[46] *NIST Chemistry WebBook*, NIST Standard Reference Database Number 69 ed., National Institute of Standards and Technology, Gaithersburg, MD.
[47] *Hands-on Manual PTR-MS 2019, Training Documentation*, IONICON Analytik GmbH, Innsbruck **2019**.

